Ca^{2+} and cAMP regulations of microtubule sliding in hyperactivated motility of bull spermatozoa

By Sumio ISHIJIMA[*1,†]

(Communicated by Tsuneyoshi KUROIWA, M.J.A.)

Abstract: To reach and fertilize the egg, mammalian spermatozoa change their flagellar movement in the female reproductive tract, named hyperactivation. The biochemical analyses of the hyperactivated movement using demembranated spermatozoa defined the factors inducing this peculiar movement; namely, large asymmetrical flagellar movement observed in the early stage of the hyperactivation was induced with a high Ca^{2+} concentration while large symmetrical flagellar movement in the late stage of the hyperactivation was generated with low Ca^{2+} and high cAMP concentrations. Under these conditions, the microtubule sliding of bull sperm flagella was investigated by disintegrating the sperm flagella with $MgATP^{2-}$ after extracting their plasma membrane and mitochondria. The large asymmetrical flagellar movement was caused by a long sliding displacement of a fiber of the doublet microtubules. On the other hand, the large symmetrical flagellar movement was generated by a large amount of microtubule sliding by many doublet microtubules.

Keywords: beat frequency, capacitation, ciliary movement, flagellar movement, metachronal sliding, synchronous sliding

Introduction

Mammalian spermatozoa change their flagellar movement during hyperactivation. Hyperactivated motility is essential for mammalian spermatozoa to reach and fertilize the egg[1] and is characterized by large bends at the proximal midpiece and low beat frequency.[2)–5)] Detailed analyses of hyperactivated flagellar movement suggest that the large bends at the proximal midpiece result from the increase in the total amount of sliding between the doublet microtubule of the sperm flagella.[3),5),6)] Furthermore, recent hydrodynamic estimation of the flagellar force calculated by the resistive-force theory using the real hyperactivated flagellar waves disclosed an important role of low beat frequency of the hyperactivated flagellar movement; namely, the slowly oscillating lateral force generated by the hyperactivated flagellar movement is most effective for sperm penetration through the zona pellucida.[7)]

To clarify the intracellular conditions under which the characteristic hyperactivated flagellar movement is generated, demembranated sperm model is useful because the effect of each chemical on the flagellar movement can be examined without changing other chemicals.[8),9)] Application of this method to the hyperactivated monkey spermatozoa revealed that highly asymmetrical flagellar movement of the early stage of the hyperactivation was caused by high levels of Ca^{2+} while large symmetrical flagellar movement of the late stage of the hyperactivation was caused by high levels of cAMP at low levels of Ca^{2+}.[10)] Since the role of Ca^{2+} and cAMP on the flagellar movement of hyperactivated spermatozoa is controversial,[10)–12)] it is necessary to clarify the effect of Ca^{2+} and cAMP on the regulatory mechanism of the microtubule sliding in activated and hyperactivated spermatozoa.

[*1] Department of Bioengineering, Tokyo Institute of Technology, Tokyo, Japan.

[†] Correspondence should be addressed: S. Ishijima, Department of Bioengineering, Graduate School of Bioscience and Biotechnology, Tokyo Institute of Technology, 2-12-1 W3-41, O-okayama, Meguro-ku, Tokyo 152-8551, Japan (e-mail: sishijim@bio.titech.ac.jp).

Abbreviations: ATP: Adenosine triphosphate; cAMP: Cyclic adenosine monophosphate; CCD: Charge-coupled device; DL: Dark low; DTT: Dithiothreitol; EGTA: Ethylene glycol tetraacetic acid; Hepes: N-2-hydroxyethylpiperazine-N′-2-ethanesulfonic acid.

doi: 10.2183/pjab.91.99

In the present study, effects of Ca^{2+} and cAMP on the flagellar movement and the microtubule sliding were investigated to clarify the microtubule sliding mechanism underlying the characteristic flagellar movement of the hyperactivated spermatozoa. The sperm flagella deprived of the plasma membrane and the mitochondria were disintegrated by sliding between the doublet microtubules with $MgATP^{2-}$. The Ca^{2+} and cAMP dependency of the microtubule sliding was compared to that of the flagellar movement, and the relationship between the flagellar movement and the microtubule sliding was investigated. Based on the results obtained from hyperactivated sperm, a flagellar microtubule sliding mechanism for activated spermatozoa is proposed. The obtained mechanism underlying the flagellar movement was identical to that proposed for the ciliary movement.

Materials and methods

Sperm preparations. Three straws (0.5 ml/straw) of frozen bull semen were thawed in a water bath for approximately 60 s at 35 °C. The highly motile spermatozoa were purified by the method of Parrish *et al.*[13] with a slight modification; namely, 1.5 ml of thawed semen was layered over a gradient of 2 ml of each of 45% and 90% Percoll (Sigma, Chemical Co., St Louis, MO, U.S.A.), and then centrifuged at 700 g for 15 min. The supernatant was removed and the sperm pellet resuspended in fresh Tyrode's solution devoid of $CaCl_2$ (8 g NaCl, 0.2 g KCl, 0.06 g $NaH_2PO_4 \cdot H_2O$, 0.1 g $MgCl_2 \cdot H_2O$, 1 g $NaHCO_3$, and 1 g glucose per liter of deionized water, pH 7.4) to make 0.3 ml concentrated sperm suspension. The spermatozoa suspended into normal Tyrode's solution swim vigorously and are referred to as activated spermatozoa.[1] The percentage of motility of these spermatozoa was 94.0 ± 1.7 (average of 385 sperm from five different experiments).

Hyperactivation by caffeine. Hyperactivation was induced by the method of Ho and Suarez;[14] namely, the concentrated sperm suspension was added to an equal volume of 20 mM caffeine (Nacalai Tesque, Inc., Kyoto, Japan) dissolved in Tyrode's solution.

Demembranation and reactivation. The obtained highly motile spermatozoa were demembranated and reactivated by the method of Ishijima *et al.*[10] with a slight modification. To remove the sperm plasma membrane, a 20 µl aliquot of the concentrated sperm suspension was added to 100 µl of extraction solution (0.2% Triton X-100, 0.2 M sucrose, 1.0 mM dithiothreitol [DTT], 25 mM potassium glutamate, 0.1 mM [ethylenebis(oxyethylenenitrilo)]tetraacetic acid [EGTA], and 40 mM N-2-hydroxyethylpiperazine-N′-2-ethanesulfonic acid [Hepes], pH 7.9) in a well of a 24-well tissue culture plate (Falcon number 3047). The suspension was stirred gently for 30 seconds, and 10 µl of the mixture transferred to 250 µl of the standard reactivation solution (0.2 M sucrose, 1.0 mM DTT, 25 mM potassium glutamate, 4 mM $MgSO_4$, 5 mM ATP, and 40 mM Hepes, pH 7.9) in another well. In experiments examining the effect of Ca^{2+} on sperm motility, Ca^{2+}-buffered reactivation solutions were used. The solutions were designed so that the concentrations of free Mg^{2+}, free ATP, and the $MgATP^{2-}$ complex remained virtually unchanged from solution to solution and were nearly identical to those in the standard reactivation solution.[10),15] In experiments to examine the effect of cAMP on sperm motility, various concentrations of cAMP were added to the Ca^{2+}-buffered reactivation solutions. Spermatozoa were freshly demembranated for each experiment. The extraction and reactivation solutions were made from stock solutions just before use. All procedures were done at room temperature (23 °C) unless otherwise noted.

Sliding disintegration of sperm flagella. Sliding disintegration of sperm flagella was performed by the method of Lindemann and Gibbons[9] with several modifications. To remove the plasma membrane and the mitochondria, a 10-µl aliquot of the concentrated sperm suspension was added to 100 µl of the extraction solution (1% Triton X-100, 0.2 M sucrose, 5 mM DTT, 25 mM potassium glutamate, 0.1 mM EGTA, and 40 mM Hepes, pH 9.5) in a well of a 24-well tissue culture plate and gently stirred and then the mixture was incubated for 5 min at 23 °C. A suspension of 10 µl was next transferred to adjacent well containing 0.25 ml of the reactivation solution. A 50-µl aliquot of the sperm suspension was then transferred to an observation chamber (0.18 mm deep, 20 mm wide, and 24 mm long) made of vinyl tape attached to the slide in two parallel strips; the trough was then covered with a glass coverslip. The removal of the mitochondria could be detected by phase-contrast microscopy as a decrease in diameter of the proximal portion of the flagella (Figs. 1, 8 and 9). To examine the process of disintegration of sperm flagella by sliding between outer doublet microtubules, an extracted sperm suspension of 10 µl was transferred to an observation chamber and then covered with a glass coverslip. The flagellar

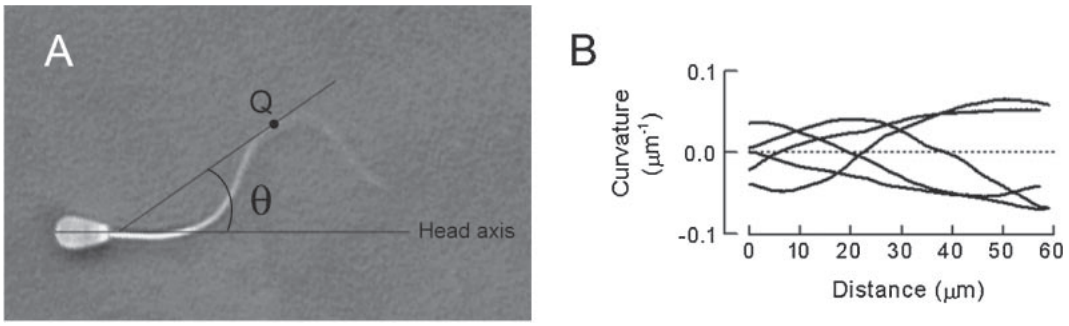

Fig. 1. Digital image analysis of flagellar beatings. **A**: The curvature of a flagellum as a function of length along the flagellum was calculated from the shear angle (θ) between the tangent to the flagellar shaft at point Q and the sperm head axis. The spermatozoa beat with three-dimensional bends because several parts of the flagella were out of focus. **B**: An example of curvature curves obtained by tracing consecutive images of a flagellum during a single beat cycle. The maximum curvature of flagellar bends is the maximum amplitude of curvature curves.

disintegration by microtubule sliding was achieved by applying 150 µl of the reactivation solution to one end of the observation chamber while the excess fluid was drained from the opposite end with small pieces of filter paper. In experiments to examine the effects of Ca^{2+} and cAMP on the flagellar disintegration, Ca^{2+}-buffered reactivation solutions and various concentrations of cAMP were also used in a similar way to the examination of flagellar movement. In this experiment, no additional elastase and trypsin was used to induce sliding of doublet microtubules.

Observations and recording. Observations were carried out using a Nikon Eclipse E600 microscope with a phase-contrast condenser and 40x BM and 100x DL objectives. To examine and record flagellar movement of spermatozoa with the 40x BM objective, a 50-µl aliquot of the sperm suspension was placed in the 0.18 mm deep observation chamber described above. To examine the three-dimensionality of flagellar movement of spermatozoa attached to a glass slide by their heads, the 100x DL objective was used because of its shallow depth of focus (approximately 0.27 µm) (Fig. 1A). For examination and recording of the disintegration of sperm flagella by microtubule sliding, the 40x BM objective was usually used, while the 100x DL objective was for more precise measurement. Images were captured directly on the memories in a computer using a Panasonic CCD video camera (WV-BL 730, Matsushita Communication Industrial Co., Ltd., Yokohama, Japan), image software (Dipp-Motion 2D, Ditect Co., Ltd., Tokyo, Japan), and a frame grabber (SIM-PCI, Ditect Co., Ltd.) at the rate of 60 images per second. The shutter speed was 1/1000 s for the flagellar movement and 1/100 s for the sliding disintegration. Observations and recording were made at 23 °C for the sliding disintegration and at 37 °C for the flagellar movement using a heated microscope stage (Thermo Plate, Tokai Hit Co., Ltd., Shizuoka, Japan).

Data analysis. For detailed field-by-field analyses, flagellar images were superimposed using image analysis software (Dipp-Motion 2D, Ditect Co., Ltd., Tokyo, Japan). Flagellar beat frequency was calculated from the period required for one complete beat. The amplitude of flagellar waves was defined as one-half of the maximum transverse displacement of the flagellum (Fig. 2). The curvature of a flagellum as a function of length along the flagellum was calculated from the shear angle between the tangent to the flagellar shaft and the sperm head axis (Fig. 1) using image analysis software (Bohboh software, Media Land Co., Ltd., Tokyo, Japan).[2),3)] Asymmetry of flagellar movement was expressed by the ratio of maximum curvature of the principal bends to that of the reverse bends at the base of the flagella.[10)] Three-dimensionality of flagellar movement of spermatozoa attached to a glass slide by their heads was determined using the fine knob of the microscope equipped with the 100x DL objective.

Statistical analysis. All data are expressed as the mean ± SD. Data were analyzed using one-way ANOVA with Scheffe post-hoc test, and Welch's t-test for examining the effect of cAMP on the number of fibers of doublet microtubules and for detecting the difference in the three-dimensionality between asymmetrical and symmetrical flagellar movement of the hyperactivated spermatozoa, using SPSS 11.0J (SPSS Japan Inc., Tokyo). The significant level was considered to be $P < 0.05$ unless otherwise noted.

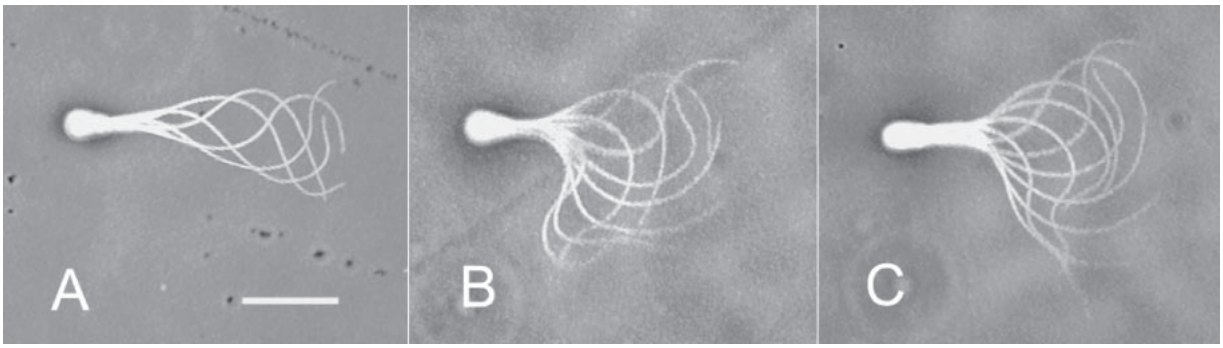

Fig. 2. Superimposed images of flagellar movement of activated and hyperactivated bull spermatozoa. The spermatozoa attach to a glass slide by their heads; thus, detailed information on the flagellar movement of individual spermatozoa is readily obtained. **A**: Activated spermatozoa. **B**: Hyperactivated spermatozoa with asymmetrical flagellar movement. **C**: Hyperactivated spermatozoa with fairly symmetrical flagellar movement. The bull spermatozoa generally beat with three-dimensional flagellar movement, but the asymmetrical flagellar movement of the hyperactivated spermatozoa is particularly out of focus (Table 1). Bar, 20 µm.

Table 1. Movement characteristics of activated and hyperactivated bull spermatozoa

	Beat frequency (Hz)	Amplitude of flagellar waves (µm)	Maximum curvature (μm^{-1})	Three-dimensionality (µm)
Activated sperm	16.3 ± 4.9^{a}	13.0 ± 3.1^{c}	0.072 ± 0.005^{f}	$1.2 \pm 1.0^{*,h}$
Hyperactivated sperm				
Asymmetrical movement	7.1 ± 1.4^{b}	22.5 ± 4.4^{d}	0.094 ± 0.011^{g}	9.9 ± 2.1^{i}
Symmetrical movement	5.2 ± 1.2^{b}	28.5 ± 3.3^{e}	0.103 ± 0.023^{g}	4.7 ± 0.9^{j}

Data were collected from more than thirty spermatozoa from four different experiments.
*The value is obtained from the direct observation of three dimensional component of the flagellar movement of spermatozoon held by its head with a micropipette.[16] [a–j]Means with different letters are significantly different.

Results

Flagellar movement of activated and hyperactivated bull spermatozoa. Superimposed images of the flagellar movement of activated and hyperactivated bull spermatozoa are shown in Fig. 2. The hyperactivated flagellar movement can be easily distinguished from the activated flagellar movement by its large bending and slow beating; namely, the activated spermatozoa had symmetrical flagellar movement with high beat frequency and small amplitude (Fig. 2A, Table 1), while the hyperactivated spermatozoa had large flagellar movement with low beat frequency and large curvature (Fig. 2B and C, Table 1). Furthermore, two types of flagellar movement can be found in the hyperactivated spermatozoa: asymmetrical flagellar movement and relatively symmetrical one (Fig. 2B and C), as reported previously.[1),2),10)] These two hyperactivated movement had different motility parameters in amplitude and three-dimensionality of flagellar waves (Table 1), suggesting different types of mechanism underlying these flagellar movement (below). In bull spermatozoa, $86.3 \pm 7.3\%$ (mean $\pm$ SD, average of 280 sperm from three different experiments) of the hyperactivated spermatozoa showed the rather asymmetrical flagellar movement and the remaining hyperactivated spermatozoa displayed the fairly symmetrical flagellar movement.

Effect of Ca^{2+} and cAMP on flagellar movement of demembranated bull spermatozoa. To identify the factor inducing the flagellar movement of hyperactivated spermatozoa, demembranated spermatozoa that were deprived of their plasma membrane with nonionic detergent Triton X-100 were used because effect of ions and other molecules on the axonemal movement could be examined directly. Both Ca^{2+} and cAMP changed the flagellar movement of demembranated, reactivated bull spermatozoa, but they produced somewhat different effects (Figs. 3–6). Ca^{2+} decreased the percentage of motile demembranated spermatozoa, while cAMP increased it (Fig. 4). Although both Ca^{2+} and cAMP changed the beat frequency of flagellar movement and the

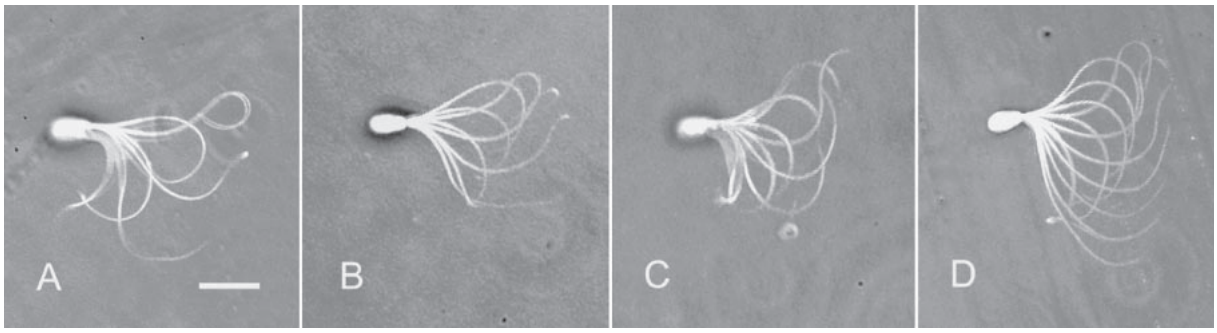

Fig. 3. Superimposed images of flagellar movement of demembranated, reactivated bull spermatozoa attached to a glass slide by their heads. The demembranated spermatozoa were reactivated with 3.5 mM $MgATP^{2-}$. Free-Ca^{2+} concentration was adjusted to be 10^{-5} M (A), 10^{-7} M (B), and 10^{-9} M (C and D). **D**: 1.0 mM cAMP was added to the reactivation solution containing 10^{-9} M Ca^{2+}. Bar, 20 µm.

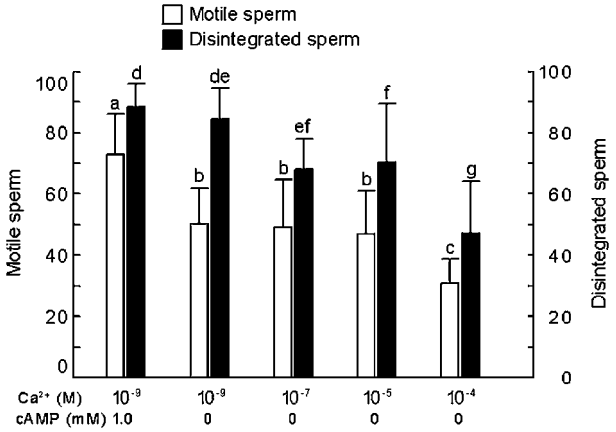

Fig. 4. Effects of Ca^{2+} and cAMP on percentage of reactivated, motile spermatozoa and disintegrated spermatozoa. Bars indicate the mean ± SD of the mean of more than 100 sperm from five different experiments. Bars with different lower case letters are significantly different.

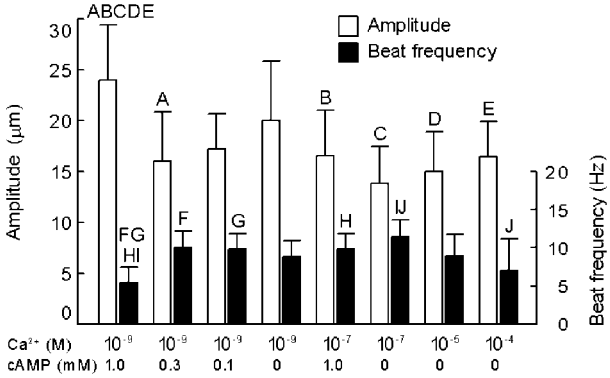

Fig. 5. Effects of Ca^{2+} and cAMP on amplitude of the flagellar waves and beat frequency of reactivated spermatozoa. Bars indicate the mean ± SD of the mean of more than thirty sperm from four different experiments. Bars with same upper case letters are significantly different.

flagellar waves (Figs. 5 and 6), decrease in Ca^{2+} concentration from 10^{-7} to 10^{-9} M increased the amplitude and decreased the beat frequency in the presence of 1 mM cAMP (Fig. 5) while Ca^{2+} increased the asymmetry of flagellar waves (Fig. 6). These results suggest that the large symmetrical flagellar movement of the hyperactivated spermatozoa is brought about by low Ca^{2+} and high cAMP while the large asymmetrical flagellar movement results from high Ca^{2+}.

Effect of Ca^{2+} and cAMP on sliding disintegration of sperm flagella. The different effects of Ca^{2+} and cAMP on the flagellar movement of demembranated spermatozoa must result from the different types of regulations of microtubule sliding. To test this hypothesis, effect of Ca^{2+} and cAMP on the sliding disintegration of the sperm flagella was examined.

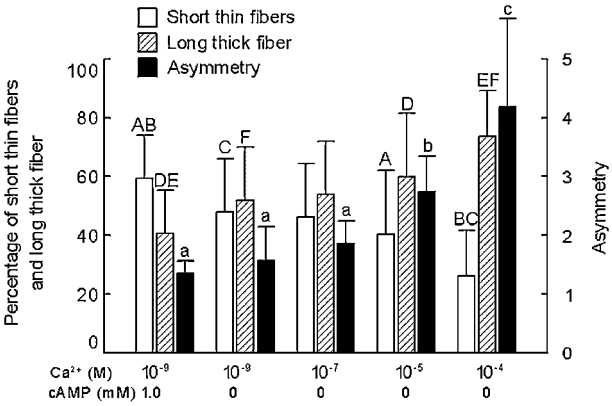

Fig. 6. Effects of Ca^{2+} and cAMP on percentage of short thin fibers and a long thick fiber, and asymmetry of flagellar waves of reactivated spermatozoa. Bars indicate the mean ± SD of the mean of more than thirty sperm from four different experiments. Bars with same upper case letters are significantly different and bars with different lower case letters are significantly different.

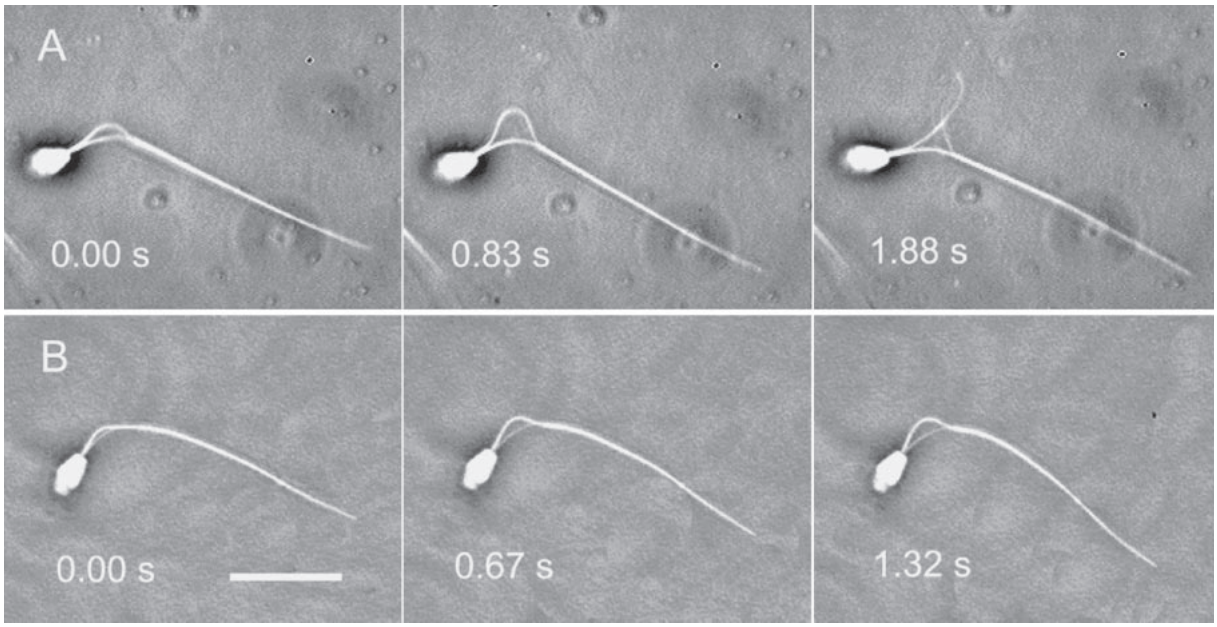

Fig. 7. Phase-contrast videomicrographs of flagellar disintegration by microtubule sliding. **A**: A thick fiber group of the doublet microtubules was extruded from the anterior end of the fibrous sheath and formed a loop at the midpiece. **B**: A thin fiber group of the doublet microtubules was separated from the sperm axoneme and formed a small bow-shape at the midpiece. These images were obtained using a 40x BM objective. Numbers indicate the time in seconds. Bar, 20 µm.

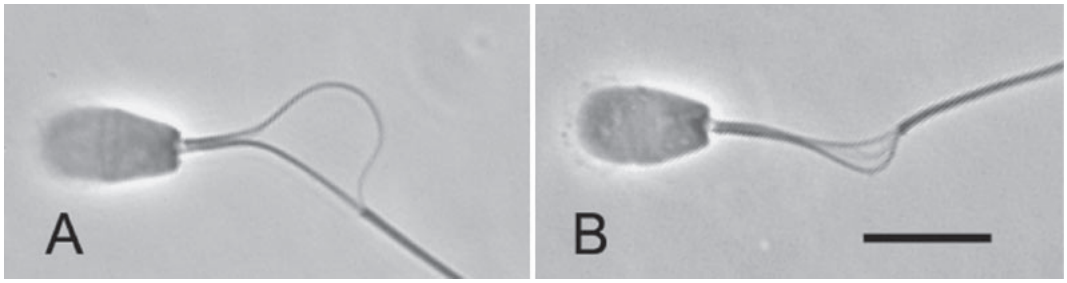

Fig. 8. Two basic patterns of flagellar disintegration by microtubule sliding. **A**: A large loop of a thick fiber group of the doublet microtubules extruded from the anterior end of the fibrous sheath. **B**: Small loops of thin fiber groups of the doublet microtubules formed at distal midpiece. These images were obtained using a 100x DL objective. Bar, 10 µm.

Ca^{2+} and cAMP had a different effect on the sliding disintegration of sperm flagella. Ca^{2+} decreased the percentage of disintegrated sperm flagella, while cAMP did not change it (Fig. 4). The effects were similar to those on the flagellar movement of demembranated spermatozoa, but the percentage of disintegration was higher than that of motile demembranated spermatozoa (Fig. 4), suggesting that Ca^{2+} and cAMP regulate the conversion of the microtubule sliding to flagellar movement.

When sperm flagella, from which the plasma membrane and the mitochondria had been extracted, were reactivated in a solution containing $MgATP^{2-}$, they normally beat for a while, stopped beating, and then began to disintegrate by sliding of the doublet microtubules. The process of the typical two examples of the sliding disintegration was shown in Fig. 7. A thick fiber of the doublet microtubules was extruded from the anterior end of the fibrous sheath and formed a loop at the midpiece (Fig. 7A). On the other hand, a thin fiber of the doublet microtubules was detached from the sperm flagella and formed a bow-shape at the midpiece (Fig. 7B). Careful observation of these disintegrations using a 100x DL objective revealed that the sliding disintegration was classified in two categories; namely, a long, thick fiber (Fig. 8A) and somewhat short, thin fibers (Fig. 8B). The former fiber hardly split into thinner ones, but

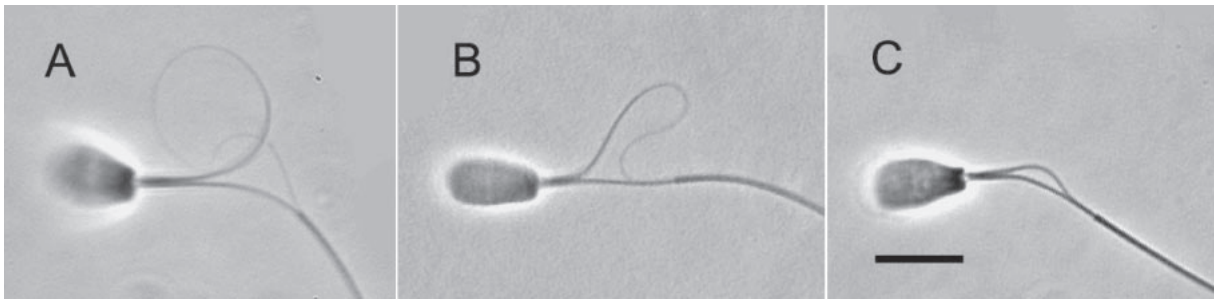

Fig. 9. Effect of Ca^{2+} on sliding displacement of doublet microtubules extruded from the sperm flagella. Free-Ca^{2+} concentration was adjusted to be 10^{-4} M (A), 10^{-7} M (B), and 10^{-9} M (C). At higher Ca^{2+} concentrations, the extruded microtubules slid entirely off the sperm flagella. Bar, 10 µm.

the latter usually disintegrated into several thin fibers. The relative frequency of occurrence of the long, thick fiber and the short, thin fibers was determined by Ca^{2+} and cAMP concentration. The long, thick fiber was observed dominantly at high Ca^{2+} concentrations, while the short, thin fibers were dominant at low Ca^{2+} and high cAMP concentrations (Fig. 6). This was mainly because the sliding displacement of extruded fibers generally reduced in size with decreasing in a Ca^{2+} concentration (Fig. 9). Furthermore, cAMP enhanced the sliding of doublet microtubules and thus increased the number of extruded fibers; namely, the percentage of the sliding disintegration consisting of more than two extruded fibers was 47.6 ± 11.6 (average of 634 sperm of four different experiments) at 10^{-9} M Ca^{2+} and 66.3 ± 12.7 (average of 587 sperm of four different experiments) at 10^{-9} M Ca^{2+} and 1.0 mM cAMP ($p < 0.01$).

Discussion

Two different types of flagellar movement of hyperactivated spermatozoa. Two different types of flagellar movement were found in the hyperactivated bull spermatozoa; namely, highly large asymmetrical flagellar movement and fairly large symmetrical flagellar movement. These two types of flagellar movement in the hyperactivated spermatozoa have been reported and analyzed in detail in the several species: golden hamster,[2] monkey,[10] and Suncus.[4] The large asymmetrical movement generates a circular swimming trajectory of the sperm head and the large symmetrical movement produces a figure-eight-path by one beat cycle because of the symmetrical movement.[2]

Various types of experiments have demonstrated that the highly asymmetrical flagellar movement is triggered by a high concentration of Ca^{2+} in the cell.[10),11),17] The present study also confirmed this fact using Ca^{2+}-buffered reactivation solutions because the components of the ATP dephosphorylation system have various effects on the flagellar movement.[15),18] On the other hand, the existence of the fairly symmetrical flagellar movement in the hyperactivated spermatozoa has not been emphasized because of its low occurrence rate in some species.[1),11),12] In fact, 50% of the motile spermatozoa of golden hamster showed the symmetrical flagellar movement in the late stage of the hyperactivation,[2] but its occurrence rate was 23.3% for monkey[10] and 13.7% for bull in the present study. However, the symmetrical flagellar movement has provided a vital clue for understanding the mechanism of the flagellar movement of spermatozoa because the large symmetrical movement of monkey spermatozoa is not induced by Ca^{2+} but by cAMP.[10] The present study confirmed this fact also for bull spermatozoa; namely, a high level of cAMP at a low Ca^{2+} concentration induced the large symmetrical flagellar movement, although 1.0 mM cAMP was needed to induce more than 70% of the large symmetrical flagellar movement for bull spermatozoa (Fig. 4) while 150 µM cAMP for monkey spermatozoa.[10] Because the occurrence rate of the large symmetrical flagellar movement of intact bull spermatozoa was only 13.7%, intracellular concentration of cAMP of the intact hyperactivated spermatozoa is undoubtedly very much lower than 1.0 mM.

Two different types of sliding disintegration by Ca^{2+} and cAMP. When the bull sperm flagella extracted the plasma membrane and the mitochondria were exposed to $MgATP^{2-}$, they were disintegrated by sliding of the doublet microtubules. No additional elastase or trypsin was necessary for inducing this disintegration because mammalian sperm flagella deprived of the plasma membrane

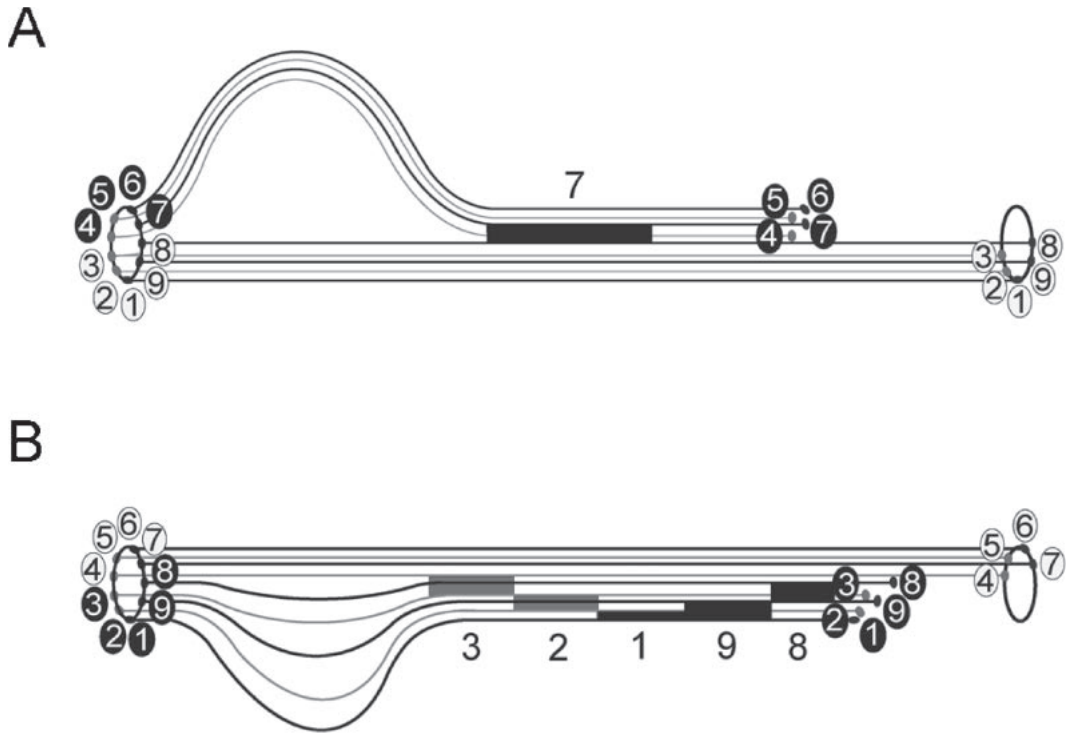

Fig. 10. Hypothec diagrams of microtubule sliding generating the hyperactivated flagellar movement. **A**: The microtubule sliding generating the asymmetrical hyperactivated flagellar movement at a high Ca^{2+} concentration. A large loop of a thick fiber group of the doublet microtubules, which may be composed of Nos. 4–7 doublet microtubules, is formed by a long synchronous sliding of No. 7 doublet microtubules. **B**: The microtubule sliding generating the symmetrical hyperactivated flagellar movement at low Ca^{2+} and high cAMP concentrations. Small loops of thin fiber groups of the doublet microtubules are formed by small number of the doublet microtubules, which independently slide between nine doublet microtubules. The numbers in the circles indicate the number of the doublet microtubules according to Afzelius.[26] The numbers indicate the sliding of corresponding doublet microtubules.

and the mitochondria are disintegrated in the presence of ATP.[9),19),20)] The sliding disintegration was classified into two basic types owing to two different types of microtubule sliding: a long, thick fiber and short, thin fibers (Figs. 7 and 8). Their occurrence rates were found to be depend on Ca^{2+} and cAMP concentrations in the present study; namely, the sliding of a long, thick fiber of doublet microtubules was induced by high Ca^{2+} concentrations while the sliding of short, thin fibers of doublet microtubules was by low Ca^{2+} and high cAMP concentrations (Fig. 6).

Ca^{2+} dependency of the microtubule sliding in mouse sperm flagella has been reported recently.[21)] However, the reactivation conditions they used did not succeed in producing the rhythmical flagellar movement of reactivated spermatozoa, and accordingly the sliding disintegration of sperm flagella in the presence or absence of 1.0 mM Ca^{2+} may not be properly assigned to their flagellar movements. In the present study, the sliding disintegration of sperm flagella was observed using the same sperm flagella after a certain period of the flagellar movement of reactivated spermatozoa. More detailed information on the microtubule sliding has been reported in sea urchin sperm flagella; namely, the extrusion of a long, thick fiber by sliding of No. 7 doublet microtubules was only found at a high Ca^{2+} concentration[22),23)] and the sliding of several doublet microtubules occurred at a low Ca^{2+} concentration.[23),24)] Furthermore, a recent investigation on the relationship between the microtubule sliding and flagellar movement of sea urchin spermatozoa revealed that various types of flagellar movement, including planar and helical movement, were induced by Ca^{2+}, cAMP, and $MgATP^{2-}$ regulation of microtubule sliding.[25)] Taking into account these results, hypothetical diagrams of flagellar disintegration by microtubule sliding are drawn (Fig. 10). The long, thick fiber consisting of Nos. 4–7 doublet microtubules is extruded by long synchronous sliding of No. 7 doublet microtubules (Fig. 10A). The sliding of a

specific pair of the doublet microtubules generates the asymmetrical movement.[25] On the other hand, the short, thin fibers generally consisting of one or two doublet microtubules are extruded by their own sliding (Fig. 10B). Each sliding displacement of individual doublet microtubules is short, but total amount of sliding displacement generated by many doublet microtubules is certainly enough to form the large flagellar movement. Furthermore, almost all doublet microtubules participate in sliding; thus, the generated flagellar movement is symmetrical.[25]

Two types of sliding between doublet microtubules are pointed out by detailed estimation of the microtubule sliding on various types of planar flagellar waves of spermatozoa: synchronous sliding and metachronal sliding.[27–30] The synchronous sliding is associated with the bend growth at the base of the flagellum while the metachronal sliding is associated with the propagation of bends of constant angle. The synchronous sliding must correspond to the sliding of long, thick fiber at a high Ca^{2+} concentration in the present study. On the other hand, the metachronal sliding is the sliding of short, thin fibers at low Ca^{2+} and high cAMP concentrations even though its two dimensional character must be extended to three dimensional one.

Microtubule sliding mechanisms of activated and hyperactivated flagellar movement of spermatozoa. At a high Ca^{2+} concentration, the large asymmetrical flagellar movement and the sliding of a long, thick fiber were induced, suggesting that the large asymmetrical movement is generated by the sliding of a long, thick fiber. On the other hand, at low Ca^{2+} and high cAMP concentrations, the large symmetrical flagellar movement and the sliding of short, thin fibers were induced, suggesting that the large symmetrical movement is produced by the sliding among many doublet microtubules. The intracellular concentration of Ca^{2+} in activated sperm flagella is approximately 10^{-8} M;[17] thus, two types of microtubule sliding must work in a sperm flagellum: the sliding of a long, thick fiber (synchronous sliding) and that of short, thin fibers (metachronal sliding). The synchronous sliding (probably by dyneins of No. 7 doublet microtubules) of a long, thick fiber generates the somewhat planar movement, while the metachronal sliding (probably by dyneins of Nos. 3–6 doublets) of short, thin fibers generates the three-dimensional movement. When intracellular concentration of Ca^{2+} increases, the synchronous sliding by No. 7 doublet microtubules extends, so that the large asymmetrical movement of the hyperactivated sperm flagella occurs. At low Ca^{2+} and high cAMP concentrations, the synchronous sliding by No. 7 doublet microtubules disappears and thus the metachronal sliding of almost all doublet microtubules begins to work, resulting in the large symmetrical movement of the hyperactivated sperm flagella. Some factors, other than Ca^{2+} and cAMP, may be involved in changing the flagellar and sliding movement because reactivated sea urchin sperm flagella beat with helical waves at low Ca^{2+} and high cAMP.[25]

The behavior of the microtubule sliding estimated by reconstructing the beating pattern of *Paramecium* cilia has been reported.[31] The pattern of microtubule sliding is essentially similar to that of flagellar movement in the present study except the feature resulted from their different length; that is, an almost planar effective stroke is generated by the synchronous sliding and three-dimensional recovery stroke is by metachronal sliding. Therefore, the same microtubule sliding mechanisms certainly function in the flagellar and ciliary movement.

In conclusion, the hyperactivated movement characterized by large and slow oscillation was generated by changing behavior of the active sliding between the doublet microtubules of the sperm flagella. Intracellular concentration of calcium and cAMP regulated these changes; namely, sliding of a long fiber of the doublet microtubules formed large asymmetrical slow oscillation at high calcium and sliding of many short fibers of the doublets made large symmetrical slow oscillation at low calcium and high cAMP. These two regulatory mechanisms of microtubule sliding by calcium and cAMP also explain the flagellar movement of intact spermatozoa, and furthermore are employed in the ciliary movement.

Acknowledgments

The author thanks Dr. Jungnickel for critically reading the manuscript.

References

1) Yanagimachi, R. (1994) Mammalian fertilization. *In* The Physiology of Reproduction (eds. Knobil, E. and Neill, J.D.). Raven Press, New York, 2nd ed., pp. 189–317.
2) Ishijima, S., Baba, S.A., Mohri, H. and Suarez, S.S. (2002) Quantitative analysis of flagellar movement in hyperactivated and acrosome-reactivated golden hamster spermatozoa. Mol. Reprod. Dev. **61**, 376–384.
3) Ohmuro, J. and Ishijima, S. (2006) Hyperactivation

is the mode conversion from constant-curvature beating to constant-frequency beating under a constant rate of microtubule sliding. Mol. Reprod. Dev. **73**, 1412–1421.
4) Kaneko, T., Mōri, T. and Ishijima, S. (2007) Digital image analysis of the flagellar beat of activated and hyperactivated Suncus spermatozoa. Mol. Reprod. Dev. **74**, 478–485.
5) Ishijima, S. (2007) The velocity of microtubule sliding: its stability and load dependency. Cell Motil. Cytoskeleton **64**, 809–813.
6) Mohri, H., Inaba, K., Ishijima, S. and Baba, S.A. (2012) Tubulin-dynein system in flagellar and ciliary movement. Proc. Jpn. Acad., Ser. B, Phys. Biol. Sci. **88**, 397–415.
7) Ishijima, S. (2011) Dynamics of flagellar force generated by a hyperactivated spermatozoon. Reproduction **142**, 409–415.
8) Gibbons, B.H. and Gibbons, I.R. (1972) Flagellar movement and adenosine triphosphatase activity in sea urchin sperm extracted with Triton X-100. J. Cell Biol. **54**, 75–97.
9) Lindemann, C.B. and Gibbons, I.R. (1975) Adenosine triphosphate-induced motility and sliding of filaments in mammalian sperm extracted with Triton X-100. J. Cell Biol. **65**, 147–162.
10) Ishijima, S., Mohri, H., Overstreet, J.W. and Yudin, A.I. (2006) Hyperactivation of monkey spermatozoa is triggered by Ca^{2+} and completed by cAMP. Mol. Reprod. Dev. **73**, 1129–1139.
11) Ho, H.-C., Granish, K.A. and Suarez, S.S. (2002) Hyperactivated motility of bull sperm is triggered at the axoneme by Ca^{2+} and not cAMP. Dev. Biol. **250**, 208–217.
12) Suarez, S.S. (2008) Control of hyperactivation in sperm. Hum. Reprod. **14**, 647–657.
13) Parrish, J.J., Krogenaes, A. and Susko-Parrish, J.L. (1995) Effect of bovine sperm separation by either swim-up or percoll method on success of in vitro fertilization and early embryonic development. Theriogenology **44**, 859–869.
14) Ho, H.-C. and Suarez, S.S. (2001) An inositol 1,4,5-trisphosphate receptor-gated intracellular Ca^{2+} store is involved in regulating sperm hyperactivated motility. Biol. Reprod. **65**, 1606–1615.
15) Okuno, M. and Brokaw, C.J. (1979) Inhibition of movement of Triton-demembranated sea-urchin sperm flagella by Mg^{2+}, ATP^{4-}, ADP and P_i. J. Cell Sci. **38**, 105–123.
16) Ishijima, S., Oshio, S., Umeda, T. and Hamaguchi, Y. (1992) Three dimensional geometry of flagellar movement of bull spermatozoa. *In* Comparative Spermatology (ed. Baccetti, B.). Raven Press, New York, pp. 387–390.
17) Suarez, S.S., Varosi, S.M. and Dai, X. (1993) Intracellular calcium increases with hyperactivation in intact, moving hamster sperm and oscillates with the flagellar beat cycle. Proc. Natl. Acad. Sci. U.S.A. **90**, 4660–4664.
18) Lesich, K.A., Pelle, D.W. and Lindemann, C.B. (2008) Insights into the mechanism of ADP action on flagellar motility derived from studies on bull sperm. Biophys. J. **95**, 472–482.
19) Olson, G.E. and Linck, R.W. (1977) Observations of the structural components of flagellar axonemes and central pair microtubules from rat sperm. J. Ultrastruct. Res. **61**, 21–43.
20) Kinukawa, M., Nagata, M. and Aoki, F. (2004) Reducing agents induce microtubule extrusion in demembranated mammalian spermatozoa. Reproduction **128**, 813–818.
21) Lesich, K.A., Kelsch, C.B., Ponichter, K.L., Dionne, B.J., Dang, L. and Lindemann, C.B. (2012) The calcium response of mouse sperm flagella: role of calcium ions in the regulation of dynein activity. Biol. Reprod. **86**, 105.
22) Sale, W.S. (1986) The axonemal axis and Ca^{2+}-induced asymmetry of active microtubule sliding in sea urchin sperm tails. J. Cell Biol. **102**, 2042–2052.
23) Ishijima, S., Kubo-Irie, M., Mohri, H. and Hamaguchi, Y. (1996) Calcium-dependent bidirectional power stroke of the dynein arms in sea urchin sperm axonemes. J. Cell Sci. **109**, 2833–2842.
24) Nakano, I., Kobayashi, T., Yoshimura, M. and Shingyoji, C. (2003) Central-pair-linked regulation of microtubule sliding by calcium in the flagellar axonemes. J. Cell Sci. **116**, 1627–1636.
25) Ishijima, S. (2013) Regulations of microtubule sliding by Ca^{2+} and cAMP and their roles in forming flagellar waveforms. Cell Struct. Funct. **38**, 89–95.
26) Afzelius, B.A. (1959) Electron microscopy of the sperm tail. Results obtained with a new fixative. J. Biophys. Biochem. Cytol. **5**, 269–278.
27) Rikmenspoel, R. (1971) Contractile mechanisms in flagella. Biophys. J. **11**, 446–463.
28) Rikmenspoel, R. (1978) The equation of motion for sperm flagella. Biophys. J. **23**, 177–206.
29) Gibbons, I.R. (1982) Sliding and bending in sea urchin sperm flagella. Symp. Soc. Exp. Biol. **35**, 225–289.
30) Brokaw, C.J. (1991) Microtubule sliding in swimming sperm flagella: direct and indirect measurements on sea urchin and tunicate spermatozoa. J. Cell Biol. **114**, 1201–1215.
31) Sugino, K. and Naitoh, Y. (1982) Simulated cross-bridge patterns corresponding to ciliary beating in *Paramecium*. Nature **295**, 609–611.

(Received July 28, 2014; accepted Jan. 15, 2015)